A R C H I V E S O F M E T A L L U R G Y A N D M A T E R I A L S
Volume 58 2013 Issue 4
DOI: 10.2478/amm-2013-0122

T. TEKER*

EFFECT OF SYNERGIC CONTROLLED PULSED AND MANUAL GAS METAL ARC WELDING PROCESSES ON MECHANICAL AND METALLURGICAL PROPERTIES OF AISI 430 FERRITIC STAINLESS STEEL

WPŁYW AUTOMATYCZNEGO I RĘCZNEGO SPAWANIA ELEKTRODĄ TOPLIOWĄ NA WŁAŚCIWOŚCI MECHANICZNE I METALURGICZNE FERRYTYCZNEJ STALI NIERDZEWNEJ AISI 430

The gas metal arc is widely used in manufacturing industries because of the high metal deposition rate and ease of automation with better weld quality at permissible cost than other welding processes in joining similar and dissimilar metals. AISI 430 steel is normally difficult to weld by melting methods, due to the associated problems such as grain growth. For this purpose, AISI 430 ferritic stainless steel couples of 10 mm thick were welded by the synergic controlled pulsed (GMAW-P) and manual gas metal arc (GMAW) welding techniques. The interface appearances of the welded specimens were examined by scanning electron microscopy (SEM). Structural changes in the weld zone were analysed by energy dispersive spectrometry (EDS) and X-ray diffraction (X-RD). Microhardness, notch charpy and tensile tests were conducted to determine the mechanical properties of specimens. Accordingly, the best result was obtained from the GMAW-P technique.

Keywords: **D.** Welding, **E.** Mechanical, **F.** Microstructure

Spawanie elektrodą topliwą w osłonie gazów aktywnych jest szeroko stosowane w przemyśle wytwórczym, ze względu na wysokie tempo osadzania metalu i łatwość automatyzacji oraz lepszą jakości spoiny przy dopuszczalnych kosztach niż w wypadku innych procesów spawania podobnych i różnych metali. Stal AISI 430 jest trudna do spawania metodami nadtapiania (z elektrodą nietopliwą), ze względu na związane z nimi problemy takie jak wzrost ziarna. Elementy ze stali ferrytycznej AISI 430 o grubości 10 mm zostały zespawane techniką GMAW-P i GMAW. Do badania morfologii spawanych próbek wykorzystano metodę skaningowej mikroskopii elektronowej (SEM). Zmiany strukturalne w strefie spoiny analizowano metodą spektrometrii z dyspersją energii (EDS) i dyfrakcji rentgenowskiej (X-RD). Pomiary mikrotwardości, udarności i próby rozciągania przeprowadzono w celu określenia właściwości mechanicznych próbek. Stwierdzono, że najlepszy wynik uzyskano dla spoin wytworzonych techniką GMAW-P.

1. Introduction

In the industry, GMAW is the most commonly used method for welding ferrous and nonferrous materials. It is a melting welding method used in both manufacturing and repairing operations [1-3]. GMAW has various advantages over other melting welding methods. High welding speed, large metal deposition, and spatter free welding are some of its advantages. In addition, it is applicable for a wide variety of commercial metals and alloys such as carbon steel, stainless steel, copper and aluminum. Furthermore, it is a mechanised method and allows robot use [2,4]. GMAW-P mode can also be regarded as wire-feed speed control of mean current. Power supply and wire-feeder are directly linked in such a way that means current is determined by wire-feed rate to ensure stable arc. The pulse waveform produced by this type of control has constant peak duration and excess current. Variable pulse parameters are peak current, base current and base current duration. This control can only be operated in the ?xed ranges of mean current as large mean current might produce multiple droplets detachments per pulse [1,5].

The current pulsing reduces overall heat input without any spatter [6]. It is a variation of constant current welding which involves cycling of the welding current from a high to a low level at a selected regular frequency [7,8]. This process works by forming one droplet of molten metal at the end of the electrode per pulse [9]. The right amount of current is then added to push that droplet across the arc and into the puddle. The detachment time is inversely proportional to the peak current magnitude [10]. In contrast to constant current welding, the heat energy required to melt the base material, supplied only during peak current pulses for brief intervals of time allows the heat to dissipate into the base material leading to a narrower HAZ. Thus, it provides “cooling off” period between subsequent pulses, which reduces the plate distortion [11]. The temperature of weld pool rises due to an exothermic reaction between argon and oxygen or carbon dioxide. In welding of steel, oxygen or carbon dioxide is mixed with argon. Therefore, oxygen accelerates the forming of low melting

* UNIVERSITY OF ADIYAMAN, FACULTY OF ENGINEERING, DEPARTMENT OF MATERIALS ENGINEERING, 02040, ADIYAMAN, TURKEY.

oxides and reduces the surface tension of metal drops falling from electrode wire. It also provides fine-grained metal structure. Carbon dioxide is decomposed into carbon monoxide and oxygen at high arc temperature. Free oxygen is combined with elements in weld pool and gives the heat back, which is gained during the decomposition. However, in this process, carbon is lost, which eventually results in decreasing hardness. Consequently, the shielding gas and its combinations are the most important parameters of GMAW method [12]. Necessity of combining materials with discrete features is due to the variety of materials in industry, the requirement of different metal joints in various processes and economic concerns [13]. Since materials to be welded have different physical, mechanical and metallurgical characteristics, welding process is more difficult than the welding of similar materials [14]. In order to have strength and continuity, a proper metal has to be chosen in welding materials with different physical and chemical properties [15]. GMAW method is also used for welding of ferritic alloys such as austenite and nickel based filler metals, other forms of stainless steel or constructional steels and other materials. Austenitic stainless steel is predominant compared to ferritic stainless steels with regard to toughness and ductility. Besides, brittleness caused by grain growth is avoided using austenitic electrode [16].

Ferritic stainless steel contains 16-30 wt.% Cr depending on alloy element. Since this steel class is easy forming, cheap and resistant against atmospheric corrosion, it is commonly used in architecture, interior and exterior decoration, food industry, wash boiler, dry machine, automotive industry and chemical industry. Normally, ferritic stainless steel has a fine grained, ductile and ferritic structure. However, in melting welding method, intergranular carbon settles and grain coarsening occurs at HAZ at temperature above 950°C. Grain coarsening and intergranular carbon precipitation negatively effect on mechanical characteristics of welding joint and such grain coarsening results in lower toughness [16-18].

Several researchers examined the effects of pulsed current on grain features at melting zone of welded joints for various materials. Ghosh et al., [19] have tried to improve weld toughness with the variation of pulse parameters in vertical-up GMAW-P. The impact toughness of melting zone and HAZ in carbon steel weld joint was found to be enhanced significantly by the refinement of its microstructure and higher ferrite content of weld metal with the increase of pulsed parameters factor φ =[(Ib/Ip)ftb].

In the present study, ferritic stainless steel material [20] that is especially used to manufacture automobile exhaust is welded by both GMAW and GMAW-P methods. Tensile, notch charpy and microhardness tests are performed to determine the strength of welded joint. In addition, microstructures developed on weld metal and heat-affected zones (HAZ) are analysed and grain morphology is examined.

2. Materials and method

Similar ferritic stainless steel (AISI 430) obtained from market, and 316L austenitic stainless steel wire of 1 mm is used in experiments. The results of chemical analyses of these materials are listed in Table 1, and mechanical properties are given in Table 2. The dimensions of specimens are 130×100×10 mm, and the specimens have 60°V welding groove. GMAW and GMAW-P was performed by MIGATRONIC KME 400 model automated welding machine. The mixture of Ar + 2%O_2 gas was used as shielding gas atmosphere. The welding speed was 4 mm/s and wire feed speed was set to 3.2 m/min. The welding voltage was 22.5 V, and a constant gas flow rate of 16 l/min was selected. Welding parameters used in this study are listed in Table 3. The welding was carried out by filling the weld groove in multi-passes (2 passes) at the top and in a single pass at the bottom for each other.

Specimens were grinded with mesh size 80-1200 for microstructure analyses and polished with 3 μm diamond paste. Then, the specimens were etched electrolytically in a solution of 50%HCl + 30%H_2O + 20%NHO_3. Microstructural changes on welding interface were examined by LEO EVO 40XVP SEM device. Microhardness measurements of specimens were carried out at an interval of 0.5 mm on load of 200 g with HV hardness scale. Lecia MHF-10 testing machine was used for measurements. EDS analysis for elementary content of phases on interface of specimens, welded by GMAW-P method, was performed using BRUKER 125 eV device. In order to determine the phases and compounds on specimens, XRD analysis was carried out through SHIMADZU XRD-6000 equipped with a Cu Kα/tube, wave length of (λ =) 1.54056 A°, voltage of 40 kV and ampere of 40 mA. Impact test specimens were prepared for the mechanical examination of the welds. ASTM E23-04 speci?cations [21] were followed for preparing and testing the impact specimens. Then the specimens were tested by using a Wolpert PW30 notch charpy test device with hammer of 300 J. Tensile test was performed in accordance with ASTM E8M-04 guidelines [22], and specimens were processed in a milling machine according to the measures listed in Figure 1. The tensile strength of specimen was determined by a Hounsfield tensile test machine with a capacity of 50000 N and 1 N accuracy and speed of 2 mm/min. In addition, SEM examined fracture surface after tensile test.

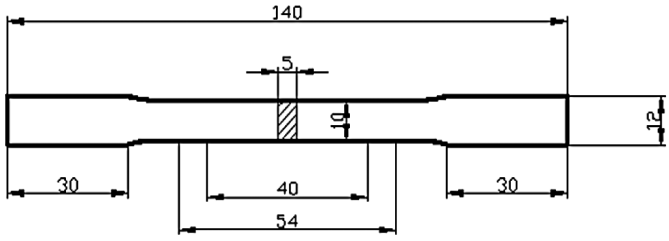

Fig. 1. Schematic illustration of tensile test specimens

3. Results and discussion

3.1. Microstructure

Photographs of internal structure of intersections taken by SEM are illustrated in Fig. 2 GMAW (S1) and Fig. 3 GMAW-P (S2). When welded joints of specimens were subjected to metallographic examination, the weld seam was observed homogeneous in appearance and ferritic stainless steel side and austenitic stainless steel weld metal exhibited different aspects. Grain coarsening was developed on welded joint

close to ferritic melting line. Then, structure turned into homogenous areas with small sized grains. Moreover, austenitic weld metal formed a symmetrical weld zone with each microstructure and a uniform weld seam was developed. The choice of the welding parameters influences the microstructure. According to Figs 2 and 3, grain coarsening on S1 specimen increased at HAZ area due to rising heat input. In a research, it was reported that high-energy input slowed down cooling and hardening, and subsequently, the resulting area had a coarsening structure [23]. Ferritic stainless steel had a fine grained and ductile structure. However, these materials tended to have grain coarsening at temperatures above 1150°C.

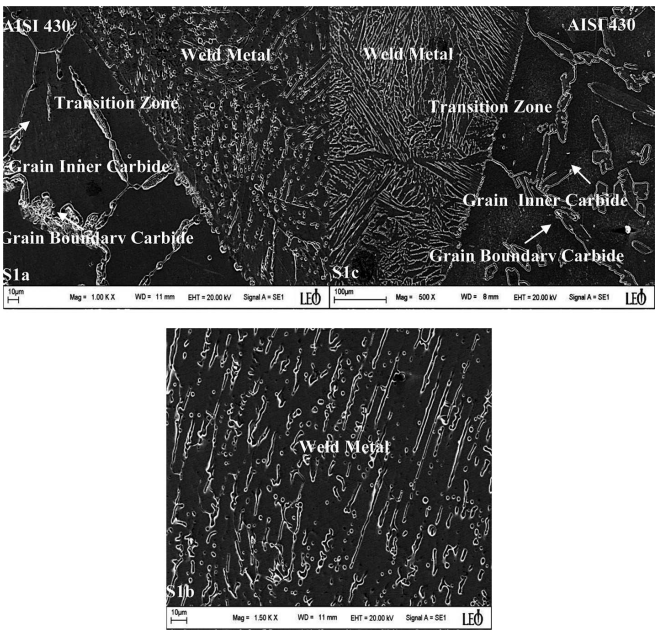

Fig. 2. SEM photograph of specimen S1: a) AISI 430 side and transition zone, b) Weld metal, c) AISI 430 side and transition zone

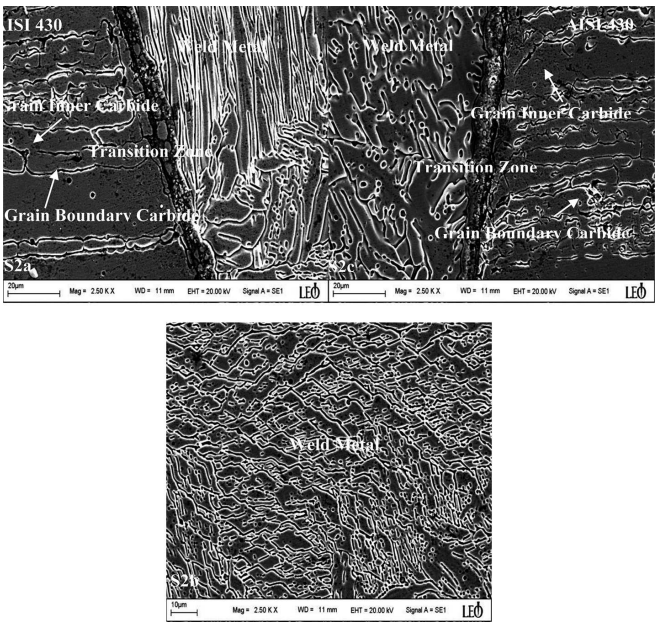

Fig. 3. SEM photograph of specimen S2: a) AISI 430 side and transition zone, b) Weld metal, c) AISI 430 side and transition zone

During welding, some part of HAZ warmed over 1150°C and grain coarsening occurred at those areas. Grain coarsening structure became brittle and the temperature increased. Since solid austenite does not transform into ferritic phase, grain size did not change [16].

There are two different microstructures for stainless steel and weld metal. Martensite (black) distribution on grain lines at weld zone and grain coarsening of ferritic grains were observed on welded joints of S1 and S2. Coarse and columnar grains on weld zone were determined in experiments performed on different materials. The reason was attributed to the high heat input and low hardening. Peppery chrome carbide (Cr_xC_y) particles were also detected to be distributed on grain lines and the area of grain coarsening. Precipitation of these carbide particles provided strength increasing, but it also caused brittleness. In Fig. 2, microstructure of joints welded by GMAW is given, while Fig. 3 illustrates the microstructure of joints welded by GMAW-P. It can also be seen from the figures that welds are different in grain size. Here, it is evident that variations of heat input directly affect the grain size of weld metal and AISI 430. Due to the low heat input in GMAW-P, weld pool have smaller area and weld metal's hardening speed increases. Reason of the variations heat input, the grain morphology and phase content in weld melting zone microstructure can be changed with different solidification modes [24]. Therefore, grains on weld metal are fine and grains at the centre of weld metal are coaxial because of the complex heat. Similar studies on weld metal demonstrated that weld metal grains moved toward heat flow. Fine-grained structure on weld metal is formed by a pulsed current [9,25,26]. Figure 3 shows the weld metal microstructure for specimen 2, which used austenitic weld metal and arc characteristics in GMAW-P, which indirectly influence the weld microstructure. The weld zone contained a dendritic microstructure with significant epitaxial growth of dendrites. The aspect ratio of the dendrites reduced to unity at the weld center. There was no significant variation of the weld microstructure in GMAW processes at a constant heat input, but the morphology of the dendrites changed with the effect of pulse parameters. The weld microstructure was found to be finer with pulsed at a given mean current, which increases the area of dendrite boundary and the amount of ferrite in the matrix. The reason of pulsing current periodic variation of arc forces occurres. Some extra fluid flows due to this generated forces which may reduce the temperature in front of the solidifying interface. The amplitude of thermal oscillations in the weld pool enhances with increasing ratio of the peak to base currents and reduces with higher pulse frequency. The temperature fluctuation inherent in pulsed welding also leads to a continuous change in the weld pool size and shape, which favors the growth of new grains. The new grains have been found to be regularly oriented toward the direction of higher thermal gradient at the interface of molten weld pool and solid base metal. Thus, the grain refinement was observed in the GMAW-P welds [25]. In Figure 4(a), a different phase is seen on the melting zone. The phase consists of 67.92% Fe, 17.68% Cr, 10.06% Ni, 0.35% C and 2.69% Mo. The composition is defined as γ-austenite according to Fe-Cr-Ni ternary phase diagram. Figure (4b) shows the SEM micrograph and EDS results of S2. The point 1 on specimen S2 consists of 59.86% Fe, 0.17% C, 29.57% Cr, 3.23% Ni and 0.87% Mo. The point 2 consists of 73.83% Fe, 0.39% C, 15.15% Cr, 0.97% Ni and 0.77% Mo. The point 3 of

specimen S2 consisting of 62.32% Fe, 0.47% C, 17.73% Cr, 9.67% Ni and 2.18% Mo. The result of EDS analyses of S2 specimen in Figure 4(b) reveals that chrome and carbon element diffusions are originated from AISI 430 ferritic stainless steel through weld metal and; on the other hand, chrome and nickel diffusions are originated from weld metal through AISI 430 steel. The phases and compounds occurred in specimens was determined by X-RD analyses. Results of X-RD analyses show that $Cr_{23}C_6$, austenite and Cr_7C_3 compounds are formed. Results are illustrated in Fig. 5.

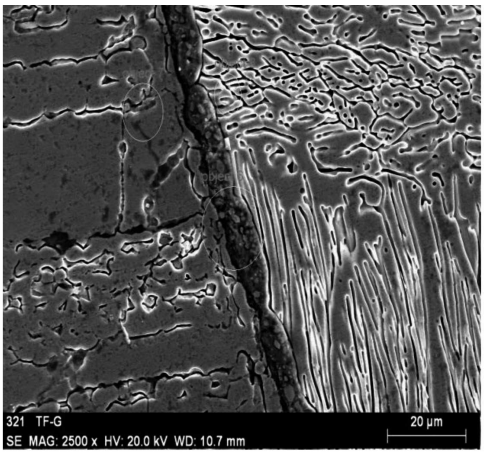

(b)

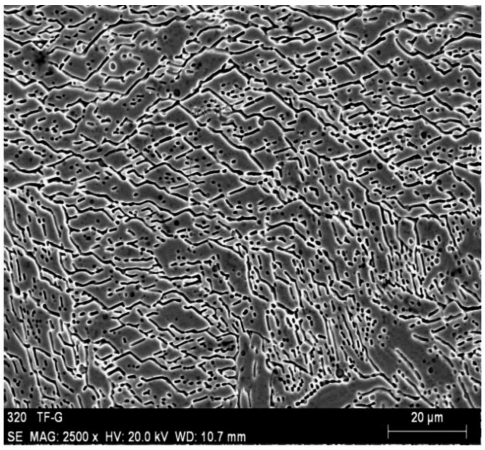

(a)

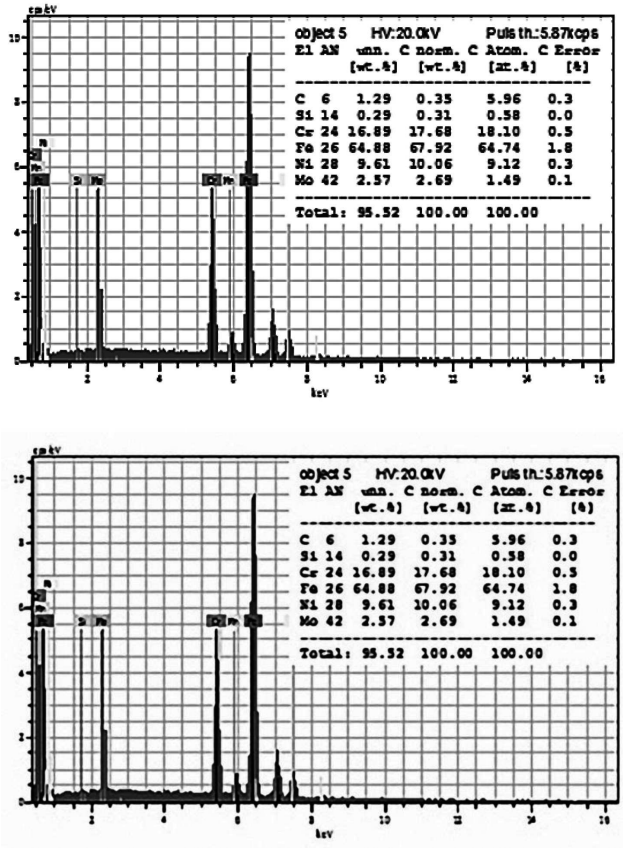

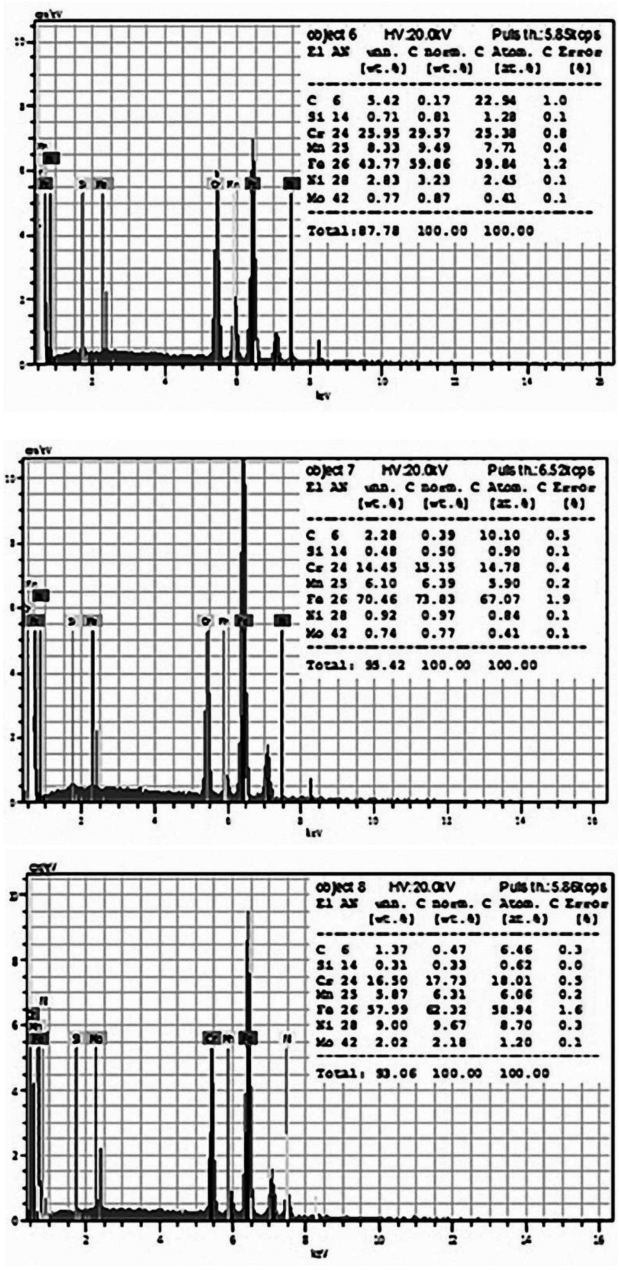

Fig. 4. EDS analyses results of S2 specimen in AISI 430 side, weld metal and transition zone

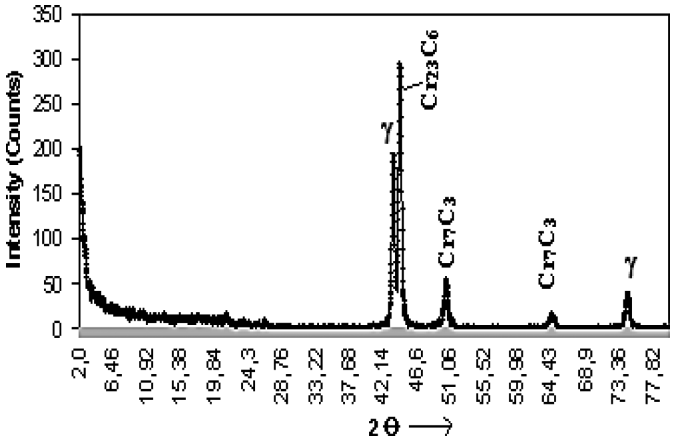

Fig. 5. X-RD graphic of specimen S2

3.2. Hardness tests

The toughness value rapidly increased at seam zone, but then it decreased to the value of main material. The microhardness analyses of welded joints on S1 and S2 are given in Fig. 6. The hardness values of S1 and S2 at welding centre are 311 HV and 385 HV, respectively. According to EDS (Fig. 4) and X-RD (Fig. 5) results, the causes of high microhardness value at weld seam were the chrome carbide phases and martensitic structure emerging due to instantaneous cooling.

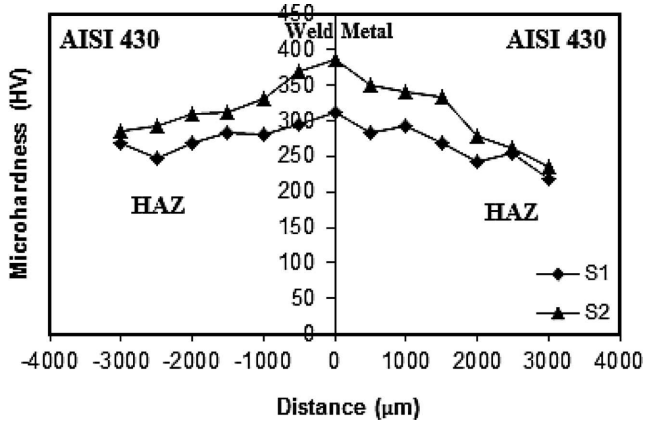

Fig. 6. Microhardness graphics of S1 and S2 specimens

Weld metal hardness obtained by GMAW-P was higher than that obtained by GMAW. Higher hardness was derived from fine grain size and instantaneous cooling. In materials grain boundary prevent the dislocation progression. Grain boundary areas in fine grain is higher than coarse grain, so that welded zone with fine grain have higher hardness than coarse grain [27]. Different hardness ratio of GMAW and GMAW-P caused by stoichiometric differences of carbide compound formation and precipitation of them. Heat input is 123-130 amperes in GMAW and 93-105 amperes in GMAW-P. Reason of this, instantaneous cooling occurred in GMAW-P. Hardness differences are caused from this. Because of higher heat input and long hardening time, coarse grains were formed and hardness value decreased on weld metal welded by GMAW method. Due to the low heat input and quick cooling, fine grains were formed on weld metal welded by GMAW-P. Therefore, hardness values of weld metal welded by GMAW-P were higher than the hardness values of weld metal formed by GMAW. Besides, stoichiometric differences of carbide precipitation and compound formation between metals had effects on the hardness value of GMAW and GMAW-P. Various experiments on different materials demonstrated that the hardness value of weld metal in synergic controlled pulsed welding method was higher due to the heat input [25,28].

3.3. Impact tests

Ferritic stainless steels (AISI 430) that are higher in chromium (16-39%) and carbon (0-12%) tend to form chromium carbides at grain boundaries in the weld heat affected zone. GMAW welded joints of ferritic stainless steel exhibited lower toughness. The refinement of grains at the weldment and increase of weld toughness are the major requirements in ferritic stainless steel weldments. In order to assess the toughness of the welded joints, notch charpy ‘v’ tests were performed. The notch charpy test results of S1 and S2 specimens at room temperature indicated that the highest charpy toughness was developed on S2 specimen with a value of 40.5 J, while the lowest value is 29 J, which was the value of S1 specimen. Normally, due to the welding heat, ferritic stainless steel exhibited coarsened grain structure at the weldment, which could be the reason for a reduction in toughness of the joints. Toughness can be regained only by refining the grain size through cold working and annealing. However, GMAW-P welded ferritic stainless steel exhibited comparatively better toughness due to the refined grain structure at weldment. On the other hand, grain coarsening was observed on S1 due to the excessive heat input. In addition, the toughness of weld seam decreases due to grain coarsening.

3.4. Tensile tests

According to the results of the tensile test, the tensile stress values of S1 and S2 are 382 N/mm^2 and 493.7 N/mm^2, respectively. During the tensile test, materials were broken on weld metal side without elongation and being wasted. Since the toughness and ductility were reduced due to grain coarsening, martensitic transition and instantaneous cooling at joint side of weldment. Both specimens were broken at AISI 430 face. Moreover, materials were determined to break at on AISI 430 side not on weld metal or at HAZ. It is proven that tensile strength of AISI 430 is lower than the tensile strength of austenitic filler metal. Austenitic stainless steel weld metal predominates compared to ferritic stainless steels with regard to toughness and ductility. In welding of different materials, strength of weld metal has to be higher than those of materials with lower strength value. The most critical area for crack initiation at welded joints is HAZ and base material interface so that the majority of the fractures and breaks are developed at this zone. During welding of ferritic stainless steel, the formation of chromium carbide in HAZ unfavourably affects the corrosion and mechanical properties of the weld joint. The reduction of the chromium carbide formation requires low heat input welding. To achieve higher strength, the heat input should be held as short as possible. Heat input in the S2 specimen welded by GMAW-P was lower than that obtained by GMAW.

3.5. Fractographs

In order to understand the behaviour of fracture the fractured surfaces were analysed by SEM. Figure 7 shows the SEM observation results on the fractured surface of the tensile test specimens. From SEM micrographs of the fractured surfaces, grains separated from specimens constituted the cavity. The cavity is uniformly distributed and different in size and shape. Crystals showed a predominantly brittle mode of fracture.

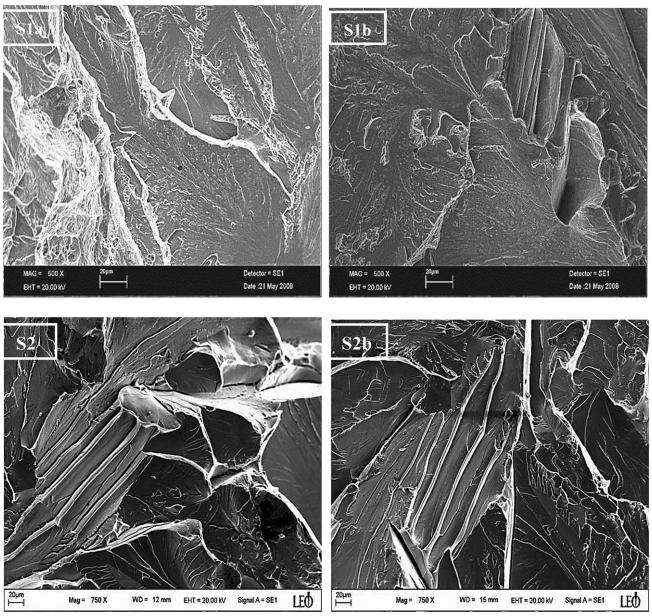

Fig. 7. SEM photograph of the fracture surface for tensile test of S1 and S2 specimens

4. Conclusion

In this study, the comparison of mechanical properties of AISI 430 steel couples welded by the GMAW-P and GMAW methods were investigated. The obtained results can be summarised as follows:

GMAW-P method can be used successfully to join ferritic stainless steel (AISI 430). The heat input of GMAW-P is lower than the heat input of GMAW. In welding of AISI 430 couple by manual welding method, it was determined that grain coarsening was formed on both sides of the weld zone and on filling metal due to the high heat input and low hardening. However, when the GMAW-P method was applied, smaller grains were formed. Therefore, synergic controlled current resulted in thinner weld metal. In both welded joints, weld metal hardness was higher compared to HAZ and the main metal. It was also observed that the grain size and heat input of weld metal obtained by GMAW were higher than GMAW-P. The maximum hardness value at welding centre was (S2= 385 HV) originated from carbide precipitation and compound forming between metals. While increasing of the heat input, carbides formation and precipitation is enhancement. This provide the dispersion strengthening, also caused the fragility in materials. The toughness of the GMAW-P welded ferritic stainless steel was comparatively higher than GMAW processed joints due to the refinement of grain size at the weld zone. Because of the high hardness values, macroscopic brittle fractures were developed on specimens. As a result of tensile test applied on welded specimens, the highest strength was obtained using the synergic controlled pulsed welding method. The processed joints exhibited better mechanical and metallurgical characteristics.

REFERENCES

[1] P. Praveen, P.K.D.V. Yarlagadda, M.J. Kang, Advancements in pulse gas metal arc welding, Journal of Materials Processing Technology **164-165**, 1113-1119 (2005).

[2] S.C. Absi Alfaro, G.C. Carvalho, S.A. Melo junior, Stand offs indirect estimation in GMAW, Mater Journal of Materials Processing Technology **3-7**, 157-158 (2004).

[3] M. Suba, J. Tusek, Dependence of melting rate in MIG/MAG welding on the type of shielding gas used, Journal of Materials Processing Technology **119**(1-3), 185-192 (2001).

[4] R. Kaçar, K. Kökemli, Effect of controlled atmosphere on the MIG-MAG arc weldment properties, Materials Design **26**(6), 508-516 (2005).

[5] P.K. Palani, N. Murugan, Selection of parameters of pulset current gas metal arc welding, Mater ProcessTechnol **172**, 1-10 (2006).

[6] M. Thamodharan, H.P. Beck, A. Wolf, Steady and pulsed direct current welding with a single converter, Welding Journal **78** (3), 75-79 (1999).

[7] A. Raja, Flux core stelliting by pulsed MAG welding, WRI J **19** (3), 98-101 (1998).

[8] I.E. French, M.R. Bosworth, A comparison of pulsed and conventional welding with basic flux cored and metal cored welding wires, Welding Journal **74** (6), 197-205 (1995).

[9] K. Pal, S.K. Pal, Effect of pulse parameters on weld quality in pulsed gas metal arc welding: A Review, Journal of Materials Engineering and Performance 2010; DOI: 10.1007/s11665-010-9717-y

[10] M. Jilong, R.L. Apps, New MIG process results from metal transfer mode control, Weld Met Fabr **51**, 168-175 (1983).

[11] B. Bernard, Effects of shielding gas in pulsed MIG welding, Join Mater, June, 277-280 (1989).

[12] A. Baggerua, Welding metallurgy. Norveç Technic University, Translates; S. Anık, Engineer: T. Tülbentçi, İskender Edit, İstanbul, 1996.

[13] V. Balasubramanian, V. Jayabalan, M. Balasubramanian, Effect of current pulsing on tensile properties of titanium alloy, Materials Design **29**, 1459-1466 (2008).

[14] V.V. Satyanarayana, G.M. Reddy, T. Mohandas, Dissimilar metal friction welding of austenitic-ferritic stainless steels, Journal of Materials Processing Technology **160** (2), 128-137 (2005).

[15] J. Tusek, Z. Kampus, M. Suban, Welding of tailored blanks of different materials, Journal of Materials Processing Technology **119** (1-3), 180-184 (2001).

[16] J.C. Lippold, D.J. Kotecki, Welding metallurgy and weldability of stainless steels, A John Wiley & Sons, Inc., Publication, 88-135 (2005).

[17] I.M. Moustafa, M.A. Moustafa, A.A. Nofal, Carbide formation mechanism during solidification and annealing of 17% Cr-ferritic steel, Mater ials Letters **42** (6), 371-379 (2000).

[18] P.K. Ghosh, S.R. Gupta, H.S. Randhawa, Characteristics of a pulsed-current, vertical-up gas metal arc weld in steel, Metallurgical Materials Transaction A **31A**, 2247-2259 (2000).

[19] J.S. Ivan, B. Paulo, P.J. Modenesi, High frequency induction welding simulating on ferritic stainless steels, Journal of Materials Processing Technology **179** (1-3), 225-230 (2006).

[20] L.M. Gourd, Principles of welding technology, Third Ed. British Library Cataloguing in Publication Data, London, 4042 (1995).

[21] ASTM International Standard E8M-04, Standard test methods for tension testing of metallic materials, 2004.

[22] ASTM International Standard E23-06, Standard test methods for notched bar impact testing of metallic materials, 2006.

[23] B. Gülenç, K. Develi, N. Kahraman, A. Durgutlu, Experimental study of the effect of hydrogen in argon as a shielding gas in MIG welding of austenitic stainless steel, International Journal of Hydrogen Energy **30** (13-14), 1475-1481 (2005).

[24] V.S.R. Murti, P.D. Srinivas, G.H.D. Banadeki, K.S. Raju, Effect of heat ınput on the metallurgical properties of HSLA steel in multi-pass MIG welding, Mater Process Technol **37**(1-4), 723-729 (1993).

[25] G. Lothongkum, E. Viyanit, P. Bhandhubanyong, Study on the effects of pulsed TIG welding parameters on delta-ferrite content, shape factor and bead quality in orbital welding of AISI 316L stainless steel plate, Journal of Materials Processing Technology **110** (2), 233-238 (2001).

[26] A. Durgutlu, Experimental investigation of the effect of hydrogen in argon as a shielding gas on TIG welding of austenitic stainless steel, Materials Design **25** (l), 19-23 (2004).

[27] W.F. Smith, Material science and engineering, Third Edition, Mc Graw-Hill Companies, 271-278 (2004).

[28] M.V. Suresh, B.V. Krishna, P. Venugopal, K. Prasad Rao, Effect of pulse frequency in gas tungsten arc welding of powder metallurgical performs, Science and Technology of welding and joining **9** (4), 362-368 (2004).

Received: 10 April 2012.